NeuroImage: Clinical 7 (2015) 273–280

Contents lists available at ScienceDirect

NeuroImage: Clinical

journal homepage: www.elsevier.com/locate/ynicl

Thalamic functional connectivity predicts seizure laterality in individual TLE patients: Application of a biomarker development strategy

Daniel S. Barron[a,b,*], Peter T. Fox[a,c,d,e,f], Heath Pardoe[g], Jack Lancaster[a,c], Larry R. Price[h,i], Karen Blackmon[g], Kristen Berry[g], Jose E. Cavazos[e,j], Ruben Kuzniecky[g], Orrin Devinsky[g], Thomas Thesen[g]

[a]Research Imaging Institute, University of Texas Health Science Center at San Antonio, San Antonio, TX, USA
[b]Yale University School of Medicine, New Haven, CT, USA
[c]Department of Radiology, University of Texas Health Science Center at San Antonio, San Antonio, TX, USA
[d]South Texas Veterans Health Care System, San Antonio, TX, USA
[e]Department of Neurology, University of TX Health Science Center, San Antonio, TX, USA
[f]State Key Lab for Brain and Cognitive Sciences, University of Hong Kong, Hong Kong
[g]Department of Neurology, New York University, New York, NY, USA
[h]College of Education, Texas State University, San Marcos, TX, USA
[i]College of Science, Texas State University, San Marcos, TX, USA
[j]San Antonio Epilepsy Center of Excellence, South Texas Veterans Health Care System, San Antonio, TX, USA

ARTICLE INFO

Article history:
Received 16 May 2014
Received in revised form 13 July 2014
Accepted 4 August 2014
Available online 7 August 2014

Keywords:
Epilepsy
Temporal Lobe Epilepsy
Thalamus
Resting-state fMRI
fMRI
Biomarker
Lateralization

ABSTRACT

Noninvasive markers of brain function could yield biomarkers in many neurological disorders. Disease models constrained by coordinate-based meta-analysis are likely to increase this yield. Here, we evaluate a thalamic model of temporal lobe epilepsy that we proposed in a coordinate-based meta-analysis and extended in a diffusion tractography study of an independent patient population. Specifically, we evaluated whether thalamic functional connectivity (resting-state fMRI-BOLD) with temporal lobe areas can predict seizure onset laterality, as established with intracranial EEG. Twenty-four lesional and non-lesional temporal lobe epilepsy patients were studied.

No significant differences in functional connection strength in patient and control groups were observed with Mann-Whitney Tests (corrected for multiple comparisons). Notwithstanding the lack of group differences, individual patient difference scores (from control mean connection strength) successfully predicted seizure onset zone as shown in ROC curves: discriminant analysis (two-dimensional) predicted seizure onset zone with 85% sensitivity and 91% specificity; logistic regression (four-dimensional) achieved 86% sensitivity and 100% specificity. The strongest markers in both analyses were left thalamo-hippocampal and right thalamo-entorhinal cortex functional connection strength. Thus, this study shows that thalamic functional connections are sensitive and specific markers of seizure onset laterality in individual temporal lobe epilepsy patients. This study also advances an overall strategy for the programmatic development of neuroimaging biomarkers in clinical and genetic populations: a disease model informed by coordinate-based meta-analysis was used to anatomically constrain individual patient analyses.

1. Introduction

Temporal lobe epilepsy (TLE) is associated with brain pathology in gray and white matter network regions connected to the epileptogenic hippocampus (Spencer, 2002). Where brain pathology most commonly occurs and whether it could be used as a disease marker are questions of long-standing interest (Bouchet and Cazauvieilh, 1825; Margerison and Corsellis, 1966; Keller and Roberts, 2008). The use of neuroimaging-based statistical biomarkers can guide the clinical evaluation of patients, particularly in complex cases without detectable lesions.

In our coordinate-based meta-analysis of medial TLE patients, we reported that the thalamus was the most common site of extra-hippocampal gray matter loss across 22 structural MRI experiments (Barron et al., 2012). This cross-study consensus informed our subsequent diffusion MRI study that reported decreased thalamo-hippocampal structural connectivity in an independent patient group (Barron et al., 2014). The present report further investigates this thalamo-hippocampal TLE model in another independent patient population using resting-state functional connectivity based on BOLD-fMRI.

* Corresponding author. at: Office of Student Affairs, 367 Cedar St, New Haven, CT 06510, USA.
E-mail address: daniel.s.barron@yale.edu (D.S. Barron).

http://dx.doi.org/10.1016/j.nicl.2014.08.002

Resting-state fMRI studies of TLE patients have reported functional connectivity changes in brain-wide analyses and anatomically constrained network models (Cataldi, Avoli and de Villers-Sidani, 2013). Such changes could inform further clinical assessment of TLE patients in terms of where to place intracranial EEG grids, particularly those without detectable lesions on structural MRIs. Previous reports have used functional connection strength to lateralize seizure onset: Bettus et al. (2010) reported an anatomically constrained network analysis within the medial temporal lobe and Morgan et al. (2012) reported a brain-wide (voxel-wise) analysis with the hippocampus (see Discussion for details). Per our previously reported TLE model, our study presents a novel, anatomically constrained network analysis of thalamic connectivity with the hippocampus, amygdala, and entorhinal cortex. To the best of our knowledge, no previous studies have evaluated an anatomically constrained model of thalamic functional connectivity.

The present study investigates the effect of TLE laterality on thalamic resting-state functional connectivity and whether thalamic connectivity has predictive value as a marker of seizure onset laterality. We compare functional connectivity strength between the thalamus, hippocampus, amygdala, and entorhinal cortex to predict whether individual patients have right or left seizure onset in separate discriminant and logistic regression analyses. Prediction efficacy is evaluated with standard performance measures and receiver operating characteristic (ROC) curves.

2. Methods

2.1. Subjects

Twenty-four right handed TLE patients (11 males, 13 females) and 20 age-matched controls were enrolled in the study from 2006 to 2013, see Table 1 for demographic information. All participants consented to the study's protocol approved by New York University's Institutional Review Board, and represent separate populations from previous work (Barron et al., 2012; Barron et al., 2014). Participants were referred for structural and functional MRI by clinicians at NYU's Comprehensive Epilepsy Center. Twenty of the 24 TLE patients were candidates for surgical resection of epileptogenic tissue, and received iEEG monitoring to confirm diagnosis and rule out additional epileptogenic areas prior to resective surgery. See Table 2 for clinical information. Each patient received a seizure onset lateralization code that was used as the "gold-standard." This lateralization code was established by iEEG when available and video EEG when unavailable. Lesions were identified through visual inspection of structural MRI by a radiologist. In addition, individual left and right hippocampal volumes were tested for significantly reduced volumes compared to a control population (see eMethods). Localization of seizure onset was determined by iEEG or video EEG. Lateralization codes based on electrophysiological recordings matched the lateralization of unilateral lesions and/or statistical hippocampal volume differences when present.

2.2. Image acquisition

Each subject underwent a single MRI session with a 3.0 T Siemens Allegra scanner. Sequences included a whole brain T1 weighted MPRAGE sequence optimized for gray–white contrast (TR/TE = 2530/3.25 ms; FA = 8°; matrix size = 256 × 256 × 128; FOV = 256 mm; voxel size = 1 × 1 × 1.3 mm^3) and a resting-state fMRI-BOLD multislice gradient-recalled echo planar imaging acquisition (TR = 2 s, FOV = 192 mm; 197 volumes, voxel size 3 × 3 × 3 mm^3) while patients lay in the scanner with their eyes open.

2.3. VOI definition

Volumes of interest (VOI) for the thalamus, hippocampus, amygdala, and entorhinal cortex were created using the Freesurfer (5.1; http://surfer.nmr.mgh.harvard.edu) recon-all function. In this procedure image volumes are resampled from native T1 image space to 1 mm isotropic space; segmentations are generated in 1 mm space then mapped

Table 1
Demographic information.

Patient	Sex	Handed[a]	Age sz onset	Sz freq. [b]	Wada language	Wada L memory	Wada R memory	GCF[c]	VCI[d]	POI[e]	WMI[f]	PSI[g]
1	F	R	17	1/m	L	10	10	Borderline impaired	77	67	—	—
2	F	R	6	2–3/m	L	5	11	Low avg	96	74	93	91
3	F	R	6	3–4/d	L	3	5	Low avg	82	103	88	93
4	F	R	32	1–2/d	—	—	—	Avg	98	96	100	102
5	F	R	—	—	L	4	11	Avg	102	105	108	94
6	M	R	—	1–4/m	L	10	12	Avg	107	102	105	108
7	F	R	5	2/y	B	4	10	Low avg	76	80	85	73
8	M	R	35	6 total	B	12	8	Avg	107	99	108	91
9	F	R	23	1/w	B	10	12	Superior	110	133	111	93
10	F	R	29	1–2/m	L	12	11	High avg	118	123	127	108
11	M	R	5	3.5/m	R	1	10	Borderline impaired	—	—	—	—
12	F	R	31	2/m	L	2	5	—	—	—	—	—
13	F	R	1	1/m	L	9	2	Avg	—	95	—	81
14	M	R	10	1–4/w	L	5	4	Superior	150	111	131	122
15	M	R	'Child'	2–3/d	L	12	0	—	—	—	—	—
16	F	R	—	3/m	L	11	5	Impaired	72	69	69	62
17	M	R	17	1/d	B	12	12	Avg	96	104	86	100
18	M	R	21	1/m	L	11	11	Low avg	75	—	86	75
19	F	R	7	0–2/m	L	11	9	Avg	109	116	91	108
20	F	R	28	3–4/w	—	—	—	Avg	125	88	114	89
21	M	R	29	2–3/w	L	12	8	Above avg	125	105	128	111
22	M	R	—	10–15/m	L	12	0	Superior	125	128	—	—
23	M	R	—	—	L	10	6	Avg	—	—	—	—
24	M	R	14 m	—	—	—	—	Impaired	76	50	55	76

[a] R = right.
[b] Self-reported, m = month, w = week, d = day.
[c] General cognitive function.
[d] Verbal comprehension index.
[e] Personal orientation inventory.
[f] Working memory inventory.
[g] Psychological screening.

Table 2
Classification of laterality and corresponding clinical information.

Patient	Laterality classification[a]	HS[b]	Lesion[c]	iEEG?	Sz onset[d]	Resection location	Engel outcome
1	Left	L	L MTS	Y	L MT	L AT, HPC	Engel 1
2	Left	L	L MTS	N	L T (vEEG)	N/A	N/A
3	Left	L	L MTS	Y	L MT	L AT, HPC	Engel 4
4	Left	L	L MTS	N	L T (vEEG)	N/A	N/A
5	Left	L	L HPC infarct	Y	L MT	L AT, HPC	Engel 1
6	Left	L	No	Y	L MT & middle TL	L Inferior AT	Engel 1
7	Left	B	No	Y	L MT	L AT, HPC	Engel 1
8	Left		No	Y	L MT	L AT, HPC	Engel 2
9	Left		No	Y	L MT	L AT, HPC	Engel 1
10	Left		L HPC & BT dysgenesis	N	L T & F (vEEG)	N/A	N/A
11	Left		L MTS	Y	L MT	L AT, HPC, AMY	Engel 1
12	Left		L T cyst	Y	L MT	L AT, HPC	Engel 1
13	Right	R	No	Y	R MT	R AT	Engel 1
14	Right	R	T gliosis	Y	R MT & R O	R AT & R O	Engel 1
15	Right	R	R MTS	Y	R MT	R AT, HPC, AMY	Engel 3
16	Right	R	R MTS	Y	R MT & mid T	R AT, HPC, AMY	Engel 2
17	Right	R	R MTS	Y	R MT	R AT, HPC, AMY	Engel 1
18	Right	B	CC & parietal hypoplasia	Y	R MT	R AT, HPC	Engel 1
19	Right		R Parietal-occipital cystic lesion	Y	R MT, R mesial O	R AT, R mesial O, & HPC	Engel 1
20	Right		R MTS	N	RT & F (vEEG)	N/A	N/A
21	Right		R PT cavernoma	Y	R MT & PT	R AT & PT cavernoma	Engel 2
22	Right		R MTS	Y	R MT, AT, & mid T	R AT, HPC	Engel 1
23	Right		No	Y	R MT	R AT, HPC, AMY	Engel 3
24	Right		No	Y	R TL & MF	No resection	N/A

Abbreviations: MTS = medial temporal sclerosis, T = temporal, O = occipital, F = frontal, AT = anterior temporal, PT = posterior temporal, M = mesial, HPC = hippocampus, AMY = amygdala, BT = basal temporal, CC = corpus callosum.
[a] Classification of laterality established by iEEG and vEEG and used in connectivity analysis.
[b] Significantly lower hippocampal volumes compared to control population.
[c] Lesions identified by radiologist's visual inspection of MRI.
[d] Localization of seizure onset established by iEEG or when unavailable, vEEG as indicated.

back onto native image space. These tools have been validated by reference to manual thalamus (Keller et al., 2012) and hippocampus (Pardoe et al., 2009) labeling in healthy subjects and epilepsy patients. Anterior and posterior hippocampal VOIs were created in individual patients by dividing the hippocampal VOI (described above) by a coronal plane at its anterior–posterior center. These anterior and posterior divisions were created to, in part, replicate the Bettus et al. (2010) study (Fig. 1).

2.4. Resting-state fMRI pre-processing

Resting-state fMRI image volumes were pre-processed according to the Weissenbacher et al. (2009) procedure by applying FSL tools within the MatLab environment. Further information may be referenced in eMethods.

2.5. Correlation, Mann–Whitney test, and effect size analysis

Mean time series signals were extracted from individual VOIs (fslmeants, implemented in MatLab) to produce 6 time series per hemisphere per subject (thalamus, hippocampus, amygdala, entorhinal cortex, anterior hippocampus, and posterior hippocampus). For each patient, *p*, and healthy control, *hc*, the Pearson product mean correlation coefficient was calculated resulting in a 12 × 12 cross correlation matrix, which was transformed to produce a Fischer *z*-score cross correlation matrix, *FC*, for each subject. These *FC* matrices represent a standardized parameter of functional connectivity and were used to investigate group differences using Mann–Whitney (Glantz, 2012) and effect size (Cohen et al., 1996) tests. Details about these tests may be referenced in eMethods.

Individual patient difference scores were calculated as individual patients' Fisher *z*-score matrix minus the control group mean Fischer *z*-score matrix ($FC_p - \bar{FC}_{hc} = Q_p$). For each patient, this yielded a 12 × 12 difference score matrix, Q_p, illustrating the difference in connection strength for connection $z_1, z_2, \ldots, z_j, \ldots z_{66}$ in a patient *p* compared to the baseline control. Difference scores were used to determine seizure onset laterality in separate discriminant and logistic regression analyses.

Data were further analyzed using discriminant and logistic regression analyses. Discriminant analysis performs group classification based on a continuous independent variable. Here, discriminant analysis classified patients as either "L" or "R" seizure onset group based on 2 difference scores of functional connectivity strength. Logistic regression is an alternative to group classification wherein the likelihood of group membership is expressed as a probability. Here, logistic regression computed the probability that a particular patient had right seizure onset (the alternative being left seizure onset) based on up to 6 difference scores. Further details about these analyses, including criteria used to select the difference scores used therein, may be referenced in eMethods. The accuracy of discriminant analysis and logistic regression was computed with standard performance measures (sensitivity, specificity, positive predictive value, and negative predictive value) and with an ROC curve (cf. Table 3 and Fig. 3).

3. Results

3.1. Group comparison: Mann–Whitney tests

Group differences in functional connection strength were evaluated with Mann–Whitney tests (Glantz, 2012). Significant group differences ($p < 0.05$, FDR correction for multiple comparisons) in functional connectivity were only observed for physiological identities, or correlations between the hippocampi and their ipsilateral (composite) anterior/posterior divisions. No other significant group differences were observed. There was a trend for R-TLE to have increased functional connectivity within left hemispheric regions while L-TLE showed decreased connectivity within left hemispheric regions. In addition, there was a general trend for the L-TLE group to have increased functional connectivity between the left thalamus and left hippocampus, between the right thalamus and left thalamus, and between the right hippocampus and left hippocampus. These trends are plotted in color as cross-correlation matrices in eFigure 1.

Table 3
Summary of discriminant and logistic regression analyses.

Patient number	HS[a]	Actual group 0 = L;1 = R	Discriminant analysis (2 predictors[b])								Logistic regression (4 predictors[c])			
			No bootstrap				Bootstrap (n = 1000)				No bootstrap		Bootstrap (n = 1000)	
			Original		Cross-validation		Original		Cross-validation					
			Group	P (p = 1)	Group	P (p = 1)	Group	P (p = 1)	Group	P (p = 1)	Group	P (p = 1)	Group	P (p = 1)
1	L	0	0	0.10	0	0.11	0	0.10	0	0.11	0	.094	0	.094
2	L	0	0	0.44	0	0.49	0	0.44	0	0.49	0	.115	0	.115
3	L	0	0	0.09	0	0.10	0	0.09	0	0.10	0	.267	0	.267
4	L	0	0	0.00	0	0.00	0	0.00	0	0.00	0	.000	0	.000
5	L	0	0	0.11	0	0.12	0	0.11	0	0.12	0	.216	0	.216
6	L	0	0	0.03	0	0.04	0	0.03	0	0.04	0	.009	0	.009
7	B	0	0	0.06	0	0.07	0	0.06	0	0.07	0	.080	0	.080
8		0	1**	0.62	1**	0.67	1**	0.62	1**	0.67	0	.475	0	.475
9		0	0	0.02	0	0.02	0	0.02	0	0.02	0	.029	0	.029
10		0	0	0.03	0	0.04	0	0.03	0	0.04	0	.016	0	.016
11		0	0	0.31	0	0.33	0	0.31	0	0.33	0	.378	0	.378
12		0	0	0.04	0	0.04	0	0.04	0	0.04	0	.035	0	.035
13	R	1	1	0.66	0**	0.17	1	0.66	0**	0.17	1	.975	1	.975
14	R	1	1	0.90	1	0.89	1	0.90	1	0.89	1	.996	1	.996
15	R	1	1	0.66	1	0.64	1	0.66	1	0.64	1	.898	1	.898
16	R	1	1	0.94	1	0.93	1	0.94	1	0.93	1	.982	1	.982
17	R	1	1	1.00	1	1.00	1	1.00	1	1.00	1	.999	1	.999
18	B	1	0**	0.17	0**	0.08	0**	0.17	0**	0.08	0**	.091	0**	.091
19		1	0**	0.21	0**	0.13	0**	0.21	0**	0.13	0**	.394	0**	.394
20		1	1	0.96	1	0.96	1	0.96	1	0.96	1	.984	1	.984
21		1	1	0.95	1	0.94	1	0.95	1	0.94	1	.968	1	.968
22		1	1	0.99	1	0.99	1	0.99	1	0.99	1	1.000	1	1.000
23		1	1	0.97	1	0.97	1	0.97	1	0.97	1	.998	1	.998
24		1	1	1.00	1	1.00	1	1.00	1	1.00	1	1.000	1	1.000

	Discriminant analysis (2 predictors[b])				Logistic regression (4 predictors[c])	
	No bootstrap		Bootstrap (n = 1000)		No bootstrap	Bootstrap (n = 1000)
	Original	Cross-validation	Original	Cross-validation		
Sensitivity	85%	79%	85%	79%	86%	86%
Specificity	91%	90%	91%	90%	100%	100%
PPV[d]	92%	92%	92%	92%	100%	100%
NPV[d]	83%	75%	83%	75%	83%	83%

[a] Hippocampal sclerosis determined by volumetric analysis, see eMethods, L = left, R = right, B = bilateral.
[b] 2 predictors = individual differences in connectivity between left thalamus and left hippocampus and between right thalamus and right entorhinal cortex.
[c] 4 predictors = individual differences in connectivity between left thalamus and left hippocampus, between right thalamus and right entorhinal cortex, between left amygdala and left amygdala, and between right posterior hippocampus and left anterior hippocampus.
[d] PPV = positive predictive value, NPV = negative predictive value, both PPV and NPV were calculated based on our sample population.

3.2. Group effects: effect size analysis

The group effect of seizure onset laterality was evaluated with standard effect size tests (Cohen et al., 1996). Medium effect sizes (>.3 as defined by Cohen (1988)) were observed for connections between the left thalamus and left hippocampus (0.43), left amygdala (0.46), and left anterior hippocampus (0.46); between the right posterior hippocampus and left hippocampus (−0.33) and left posterior hippocampus (−0.33); between the right thalamus and left amygdala (0.34); and between the right entorhinal cortex and right thalamus (−0.30) (See Fig. 2 and eTable 2).

Six connections met our criteria for suitable predictors of seizure onset laterality. These connections are described below in reference to their usage in the discriminant and logistic regression analyses. The selection criteria for these connections are explained in eMethods and are presented in tabular form in eTable 3.

3.3. Group classification: discriminant analysis

A direct discriminant analysis was performed using 2 functional connection strengths to determine group classification. The 2 functional connections were between the left thalamus and left hippocampus (modeled as "predictor 1") and between the right entorhinal cortex and the right thalamus (modeled as "predictor 2"). Individual patients were classified into right (modeled as "1") and left (modeled as "0") seizure onset groups. One discriminant function was generated ($\lambda = .42$; χ^2 (2, N = 24) = 18.2; $p < .001$) and indicated that the function of the predictors significantly differentiated between patients' laterality. Group classification (laterality) explained 100% of function variance. Predictor 1 was most associated with the function (e.g., 1.123 — standardized function. 57 — correlation with discriminant function).

Discriminant analysis predicted seizure onset laterality with a sensitivity of 85% and a specificity of 91% (cross-validation of the discriminant analysis was similar: 79% sensitivity, 90% specificity). For the sample, 87.5% of the original cases were correctly classified and 83% of the cases were correctly classified in the cross-validation analysis, described in eMethods. An ROC curve showed that the discriminant analysis of original cases was significantly different from a completely random group assignment ($p < .0001$). Cross-validation analysis was also significant ($p < .001$). Individual patient results, additional performance measures, discriminant analysis parameter estimates, and standard errors for the bootstrap analysis are reported in Table 3. See Fig. 3 for full ROC parameters.

3.4. Group probability: logistic regression analysis

Six logistic regression analyses were performed using 1 through 6 functional connection strengths to predict the probability of seizure onset laterality. The logistic regression with four predictors yielded the most reliable parameter estimates, with the standard error for each predictor being less than 4.2. These four predictors represented connectivity strength between the: left thalamus and left hippocampus,

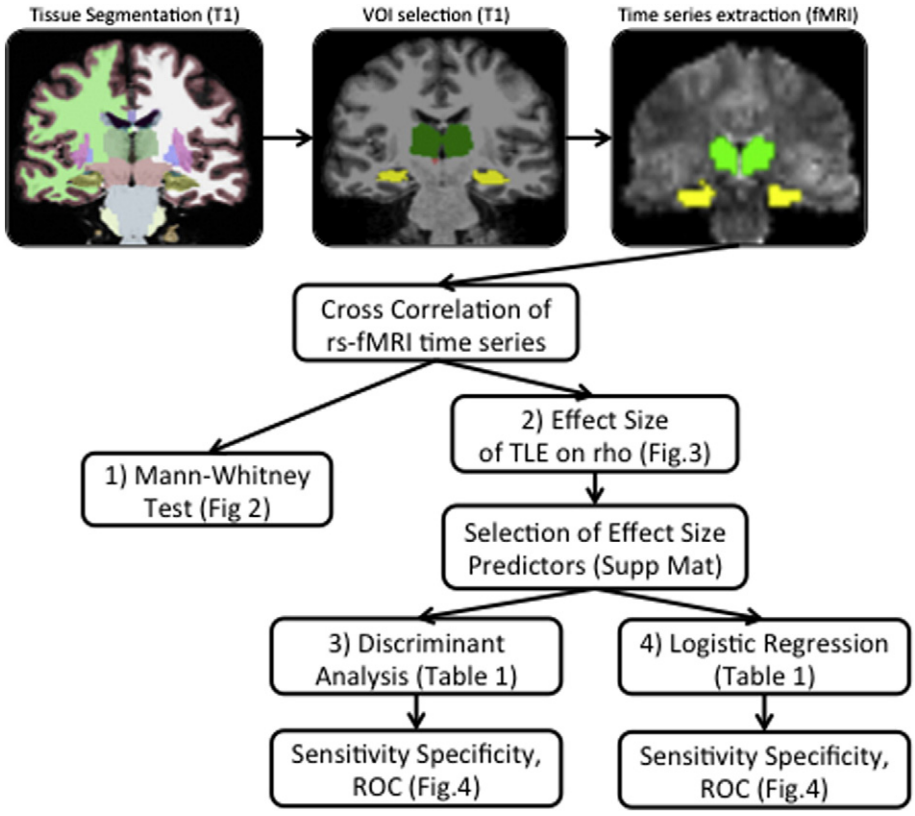

Fig. 1. Analysis overview. Individual subject structural MRI image volumes were segmented and the thalamus, hippocampus, amygdala, and entorhinal cortex volumes of interest (VOIs) were transformed to functional MRI space. Within these VOIs, mean time series were extracted and cross correlations were computed. 1) Group comparisons were performed with Mann–Whitney tests. 2) The effect size of individual patient's TLE on rho was compared to corresponding mean of healthy controls ($n = 20$). 3) Discriminant analysis and 4) logistic regression were performed to predict seizure onset laterality from functional connectivity effect size. Selection of effect size predictors is described in eMethods and supplementary materials.

modeled as "predictor 1"; right thalamus and right entorhinal cortex, "predictor 2"; right amygdala and left hippocampus, "predictor 3"; and right posterior hippocampus and left anterior hippocampus, "predictor 4". Based on the Wald criterion at the four predictor logistic regression, only "predictor 2" was significant ($p = 0.05$). Lack of significance was due to large standard errors of estimated beta weights as a byproduct of performance of the maximum likelihood estimator under small sample size (Keller et al., 2014; Hosmer et al., 2013). See eTable 4 for a summary of difference scores utilized and parameters from all six logistic regressions including regression coefficients, Wald statistics, odds ratios, and 95% confidence intervals for odds ratios.

A test of the full model with four predictors against a constant-only model was statistically significant, χ^2 ($df = 4$, $N = 24$) $= 22.064$, $p < .001$, indicating that as a set, the predictors reliably distinguished between R and L TLE patients. The variance accounted for in classification was large, Nagelkerke $R = .802$. These four connections predicted

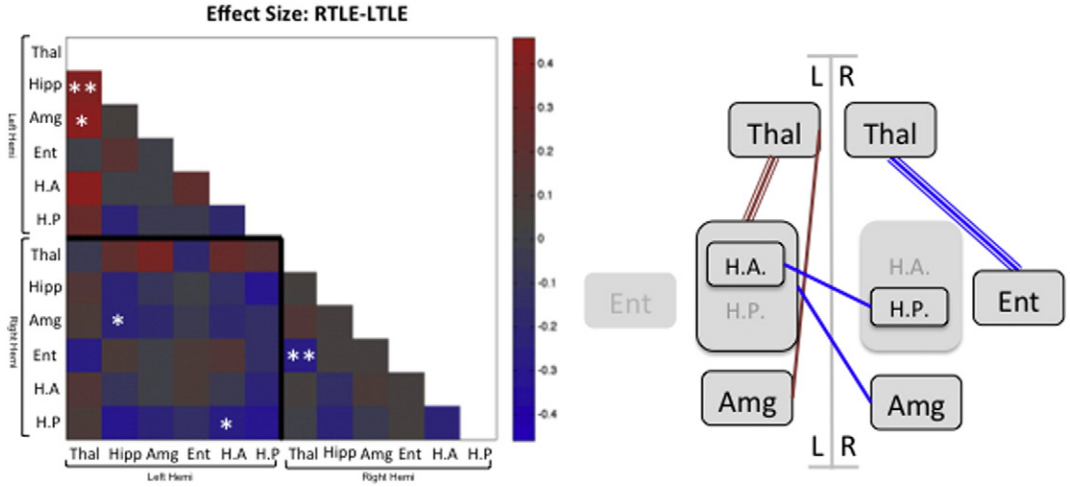

Fig. 2. Effect size of TLE laterality on functional connectivity. Left: effect size was calculated as the difference of group averaged Fischer transformed correlation coefficients for R (red) and L (blue) TLE patients subtracted from the control group mean (Cohen, 1988). Effect sizes used as predictors for discriminant analysis are denoted with * and those used for logistic regression denoted with both * and **. To improve clarity of the figure, the redundant upper triangle of the matrix has been excluded. Right: diagram of effect sizes used to predict seizure onset laterality. Red lines represent increased functional connectivity compared to control; blue lines represent decreased. Triple lines represent effect sizes used in discriminant analysis; logistic regression used both triple and single lines.

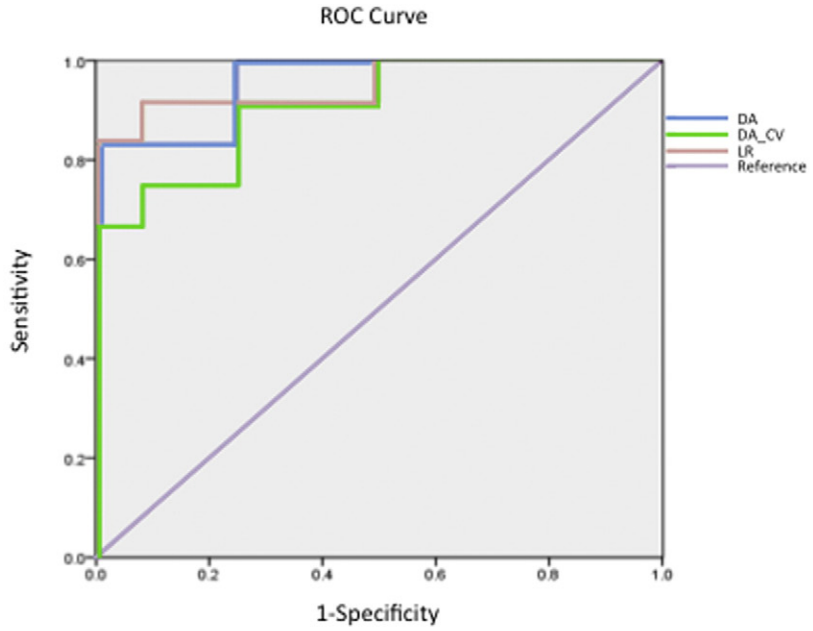

	Test Result Variable(s)	Area	Std. Error[a]	P Value (Asymptotic)[b]	95% CI Lower Bound	95% CI Upper Bound
2 Predictors	Discriminant Analysis (DA)	.958	.037	.000	.887	1.000
	Discriminant Analysis Cross Validation (DA_CV)	.910	.058	.001	.796	1.000
4 Predictors	Logistic Regression (LR)	.951	.045	.000	.864	1.000

a. Under the nonparametric assumption
b. Null hypothesis: true area = 0.5

Fig. 3. ROC curve of discriminant and logistic regression analysis methods. Curve is based on individual patient data reported in Table 3. Discriminant analysis probabilities were adjusted to be relative to diagnosis of RTLE, P ($p = 1$).

laterality with a sensitivity of 86% and a specificity of 100% (other performance characteristics, see Table 3 & Fig. 3). Notwithstanding the small sample size, analyses with and without bootstrapping achieved identical results. Individual patient laterality predictions can be referenced in Table 3.

4. Discussion

This study demonstrates that inter-regional resting-state functional connectivity predicts the hemisphere of seizure onset in individual TLE patients. Consistent with our previously proposed network model of TLE, the strongest predictors of seizure onset laterality were connectivity strength between the left thalamus and left hippocampus and between the right thalamus and right entorhinal cortex. Using these connection strengths, discriminant analysis and logistic regression predicted seizure onset laterality with high sensitivity and specificity.

4.1. Anatomically constrained analyses outperform brain-wide analyses

Using a novel strategy and statistical method, we found that thalamic connectivity was the strongest predictor of seizure onset in patients with TLE. Our goal was to determine which network connections would be most affected by TLE laterality and therefore be most predictive of seizure onset laterality. Based on a previously proposed (Barron et al., 2012) and confirmed (Barron et al., 2014) thalamic model of TLE network damage, this study performed a functional connectivity analysis between the thalamus, hippocampus, amygdala, and entorhinal cortex.

Bettus et al. (2010) reported an anatomically constrained analysis that detected TLE-related changes in functional connections between the posterior hippocampus and amygdala and between the anterior hippocampus and posterior hippocampus. These connection strengths lateralized seizure onset zone with 64% sensitivity and 91% specificity. For this reason, the amygdala, entorhinal cortex, and anterior and posterior hippocampal divisions were included as seeds in our analysis of thalamic connectivity.

Morgan et al. (2012) reported a brain-wide (voxel-wise) functional connectivity analysis between the whole hippocampus and each brain voxel. Altered connectivity between the right hippocampus and 5 thalamic voxels lateralized the seizure onset zone with 100% sensitivity and 87.5% specificity in 7 patients. We attempted to replicate this analysis in our 23 patient sample by analyzing hippocampal connectivity in two ways: first to each thalamic voxel (as in Morgan et al., 2012) and then to each thalamic nucleus (as defined in Krauth et al., 2010). In both analyses, individual patient difference scores varied greatly and were not consistently predictive of laterality. We observed that the smaller the volume analyzed, the more variable the measurement across subjects (data unreported). That is, the voxel-wise analysis performed less well than the per-nucleus analysis, which performed less well than the regional-thalamus analysis (reported here).

4.2. Framework for thalamic involvement in TLE

Because thalamic connections were the most predictive of TLE laterality, we now propose a framework for thalamic involvement in TLE. Thalamic involvement in TLE seizure initiation (Spencer, 2002), propagation (Guye, 2006), and spread (Bertram et al., 2008) is supported by a large and growing literature. Thalamic atrophy is correlated to medial temporal lobe (MTL) atrophy in volumetric (Bernhardt et al., 2012), diffusion tractography (Keller et al., 2014), and T2 weighted studies (Keller et al., 2014). In comparison to neocortical atrophy, thalamic atrophy is relatively uncorrelated to disease duration (Coan et al., 2014). Together, these observations imply that thalamic involvement differs with disease progression and suggests stage-specific

involvement of thalamic nuclei. The thalamic medial dorsal nucleus is the most consistent site of gray matter reduction reported in structural MRI studies (Barron et al., 2012), suggesting that the medial dorsal nucleus represents an early "damaged" pathway in TLE. Notwithstanding decreased thalamic structural connectivity with the temporal lobe in medial TLE patients (Keller et al., 2014), the medial pulvinar remained the most structurally connected thalamic nucleus (Barron et al., 2014), suggesting that the medial pulvinar represents a consistently "open" pathway.

Given the observations of midline thalamic atrophy (Bernhardt et al., 2012), we propose that epileptogenic damage to the anterior and medial dorsal nuclei facilitates TLE seizure onset (per Coan et al., 2014)), while damage to the medial pulvinar facilitates seizure generalization (Rosenberg et al., 2009). Such a framework provides further anatomical basis for the concept that network disruption (as opposed to a single, focal disruption) causes seizures (Cavazos and Cross, 2006). Neuroimaging supports this framework, however, definitive nucleus-specific electrophysiological studies are required as a formal validation.

4.3. Interpretation of predictors

Thalamo-hippocampal functional connection strength was the strongest predictor of seizure onset laterality in both our discriminant analysis and logistic regression analysis. Thalamo-entorhinal cortex connection strength was the second strongest predictor. Both of these novel findings are consistent with known physiology, as follows.

Physiological synchronization between the thalamus and MTL structures has been described during TLE seizure (electrophysiology (Guye, 2006)) and at rest (fMRI (Cataldi et al., 2013)). The entorhinal cortex is the main excitatory input to the hippocampus and is known to significantly interact with the hippocampus at seizure onset (Guye, 2006; Bartolomei et al., 2005), likely via CA1 and subicular hippocampal connections, which reorganize during epileptogenesis (Cavazos and Cross, 2006; Witter, 1993). Ictal electrophysiological synchronization of the entorhinal cortex with the thalamus occurs before hippocampal synchronization with the thalamus, suggesting that whatever influence the thalamus exerts on the hippocampus acts via the entorhinal cortex (Guye, 2006).

For both predictors, no comparable effects in the opposite hemisphere were observed, i.e. left thalamo-hippocampal connectivity was increased in L compared to R-TLE patients but right thalamo-hippocampal connectivity was not increased in R compared to L-TLE patients. One explanation could be that R and L-TLE affect network connectivity in different ways, as demonstrated by Bernhardt et al. (2011) and Karunanayaka et al. (2011). Another explanation could be that left and right thalamo-hippocampal connections are differentially engaged during the resting state. The presence of lateralized attention (right hemisphere) and language (left hemisphere) networks during the resting state supports this idea. While neuropsychological measures of language ability are known correlates of L-TLE, the relation of R-TLE to attention set switching and maintenance is relatively unknown. Further investigation of these measures in relation to functional connectivity strength could therefore prove useful.

4.4. Biomarker discovery

The strategy and results presented seek to identify a biomarker using an anatomically constrained model of TLE. It is notable that while multiple differences in connection strength were useful predictors of seizure onset laterality, no one connection significantly differed from controls in group-level comparisons. In terms of biomarker identification, our results argue that the absence of a significant group-level difference should not discourage efforts to assess the clinical utility of multiple differences at the individual-level. Such an approach may be optimized when investigating the predictive effects of a disease model informed by coordinate-based meta-analysis, as done here.

4.5. Limitations

Functional connectivity is an operative term applied to temporally correlated, spatially remote neurophysiological events (Friston, 1994). As applied here, functional connectivity represents temporal correlations in the mean fMRI-BOLD time-series signal of particular tissue volumes acquired under the resting condition. While functional connectivity is not intended to imply structural connectivity, our results are consistent with previous reports investigating structural connectivity (Barron et al., 2014; Keller et al., 2014).

Although the patient sample studied ($n = 24$) is relatively large for an fMRI study, a larger cohort would increase the rigor of these results. Because of concerns about small sample size, we performed discriminant analysis and logistic regression with and without bootstrapping ($n = 1000$); identical results were achieved. We addressed concerns of model "over-fitting" in the discriminant analysis by inclusion of a leave-one-out cross-validation. This step yielded a small decrease in prediction performance, however served as a validation of the specific analytic model built and used in the discriminant analysis. While the overall strategy of building a disease model with coordinate-based meta-analysis may reasonably be tested in other neurological disorders, the specific disease model tested in the present analysis is specific to the TLE population. As such, the sensitivity and specificity metrics reported above are limited to the TLE population.

Notwithstanding these limitations, the present study further confirms our previously proposed TLE disease model in an independent patient population using different methods.

5. Conclusion

Thalamic functional connectivity can predict seizure onset laterality in TLE patients with and without hippocampal sclerosis. This study advances an overall strategy for the programmatic development of neuroimaging biomarkers in clinical and genetic populations: a disease model informed by coordinate-based meta-analysis was used to anatomically constrain individual patient analyses.

Conflict of interests disclosure

None reported.

Funding/support

Funding from the National Institute of Neurological Disorder & Stroke1-F31-NS083160-01 (D.S.B.), National Institute of HealthRO1 MH074457 (P.T.F.), F.A.C.E.S (Finding a cure for epilepsy and Seizures; T.T., O.D.) and the American Epilepsy Foundation (T.T.) assisted in the collection, management, analysis, and interpretation of the data; and in the preparation and review of the manuscript.

Acknowledgments

The authors thank Kristin S. Budde (BA, MD, MPH, Yale University) for her review of the manuscript; Xiuyuan Wang (BS, MS, New York University) for his technical assistance with MatLab; and Callah Boomhaur (BA, New York University) for her administrative assistance. Daniel S. Barron had full access to all of the data in the study and takes responsibility for the integrity of the data and the accuracy of the data analysis.

Supplementary material

Supplementary material for this article can be found online at http://dx.doi.org/10.1016/j.nicl.2014.08.002.

References

Barron, D.S., Fox, P.M., Laird, A.R., Robinson, J.L., Fox, P.T., 2012. Thalamic medial dorsal nucleus atrophy in medial temporal lobe epilepsy: a VBM meta-analysis. NeuroImage. Clinical 2, 25–32. http://dx.doi.org/10.1016/j.nicl.2012.11.00424179755.

Barron, D.S., Tandon, N., Lancaster, J.L., Fox, P.T., 2014. Thalamic structural connectivity in medial temporal lobe epilepsy. Epilepsia 2014, e50–e55. http://dx.doi.org/10.1111/epi.1263724802969.

Bartolomei, F., Khalil, M., Wendling, F., et al., 2005. Entorhinal cortex involvement in human mesial temporal lobe epilepsy: an electrophysiologic and volumetric study. Epilepsia 46 (5), 677–687. http://dx.doi.org/10.1111/j.1528-1167.2005.43804.x15857433.

Bernhardt, B.C., Chen, Z., He, Y., Evans, A.C., Bernasconi, N., 2011. Graph-theoretical analysis reveals disrupted small-world organization of cortical thickness correlation networks in temporal lobe epilepsy. Cerebral Cortex (New York, N.Y.: 1991) 21 (9), 2147–2157. http://dx.doi.org/10.1093/cercor/bhq29121330467.

Bernhardt, B.C., Bernasconi, N., Kim, H., Bernasconi, A., 2012. Mapping thalamocortical network pathology in temporal lobe epilepsy. Neurology 78 (2), 129–136. http://dx.doi.org/10.1212/WNL.0b013e31823efd0d22205759.

Bertram, E.H., Zhang, D., Williamson, J.M., 2008. Multiple roles of midline dorsal thalamic nuclei in induction and spread of limbic seizures. Epilepsia 49 (2), 256–268. http://dx.doi.org/10.1111/j.1528-1167.2007.01408.x18028408.

Bettus, G., Bartolomei, F., Confort-Gouny, S., et al., 2010. Role of resting state functional connectivity MRI in presurgical investigation of mesial temporal lobe epilepsy. Journal of Neurology, Neurosurgery, and Psychiatry 81 (10), 1147–1154. http://dx.doi.org/10.1136/jnnp.2009.19146020547611.

Bouchet, M.M., Cazauvieilh, J.B., 1825. De l'epilepsie consideree dans ses rapports avec l'alienation mentale. Archives. générales de Médecine 9, 510–542.

Cataldi, M., Avoli, M., de Villers-Sidani, E., 2013. Resting state networks in temporal lobe epilepsy. Epilepsia 54, 2048–2059. http://dx.doi.org/10.1111/epi.1240024117098.

Cavazos, J.E., Cross, D.J., 2006. The role of synaptic reorganization in mesial temporal lobe epilepsy. Epilepsy & Behavior: E&B 8 (3), 483–493. http://dx.doi.org/10.1016/j.yebeh.2006.01.01116500154.

Coan, A.C., Campos, B.M., Yasuda, C.L., et al., 2014. Frequent seizures are associated with a network of gray matter atrophy in temporal lobe epilepsy with or without hippocampal sclerosis. PloS One 9 (1), e85843. http://dx.doi.org/10.1371/journal.pone.008584324475055.

Cohen, J., 1988. Statistical Power Analysis for the Behavioral Sciences, second edition. Lawrence Eribaum Associates.

Cohen, M.S., Kosslyn, S.M., Breiter, H.C., et al., 1996. Changes in cortical activity during mental rotation. A mapping study using functional MRI. Brain: A Journal of Neurology 119 (1), 89–1008624697.

Friston, K.J., 1994. Functional and effective connectivity in neuroimaging: a synthesis. Human Brain Mapping 2 (1–2), 56–78.

Glantz, S.A., 2012. Primer of Biostatisticsseventh edition. McGraw-Hill.

Guye, M., 2006. The role of corticothalamic coupling in human temporal lobe epilepsy. Brain: A Journal of Neurology 129 (7), 1917–1928. http://dx.doi.org/10.1093/brain/awl15116760199.

Hosmer, D.W., Lemeshow, S., Sturdivant, R.X., 2013. Applied Logistic Regressionthird edition. Wiley, Hoboken, NJ.

Karunanayaka, P., Kim, K.K., Holland, S.K., Szaflarski, J.P., 2011. The effects of left or right hemispheric epilepsy on language networks investigated with semantic decision fMRI task and independent component analysis. Epilepsy & Behavior: E&B 20, 623–632. http://dx.doi.org/10.1016/j.yebeh.2010.12.02921273134.

Keller, S.S., Gerdes, J.S., Mohammadi, S., et al., 2012. Volume estimation of the thalamus using Freesurfer and stereology: consistency between methods. Neuroinformatics 10 (4), 341–350. http://dx.doi.org/10.1007/s12021-012-9147-022481382.

Keller, S.S., O'Muircheartaigh, J., Traynor, C., Towgood, K., Barker, G.J., Richardson, M.P., 2014. Thalamotemporal impairment in temporal lobe epilepsy: a combined MRI analysis of structure, integrity, and connectivity. Epilepsia 55, 306–315. http://dx.doi.org/10.1111/epi.1252024447099.

Keller, S.S., Roberts, N., 2008. Voxel-based morphometry of temporal lobe epilepsy: an introduction and review of the literature. Epilepsia 49 (5), 741–757. http://dx.doi.org/10.1111/j.1528-1167.2007.01485.x18177358.

Krauth, A., Blanc, R., Poveda, A., Jeanmonod, D., Morel, A., Székely, G., 2010. A mean three-dimensional atlas of the human thalamus: generation from multiple histological data. NeuroImage 49 (3), 2053–2062. http://dx.doi.org/10.1016/j.neuroimage.2009.10.04219853042.

Margerison, J.H., Corsellis, J.A., 1966. Epilepsy and the temporal lobes. A clinical, electroencephalographic and neuropathological study of the brain in epilepsy, with particular reference to the temporal lobes. Brain: A Journal of Neurology 89 (3), 499–5305922048.

Morgan, V.L., Sonmezturk, H.H., Gore, J.C., 2012. Lateralization of temporal lobe epilepsy using resting functional magnetic resonance imaging connectivity of hippocampal networks. Epilepsia 53 (9), 1628–1635. http://dx.doi.org/10.1111/j.1528-1167.2012.03590.x22779926.

Pardoe, H.R., Pell, G.S., Abbott, D.F., Jackson, G.D., 2009. Hippocampal volume assessment in temporal lobe epilepsy: how good is automated segmentation? Epilepsia 50 (12), 2586–2592. http://dx.doi.org/10.1111/j.1528-1167.2009.02243.x19682030.

Rosenberg, D.S., Mauguière, F., Catenoix, H., Faillenot, I., Magnin, M., 2009. Reciprocal thalamocortical connectivity of the medial pulvinar: a depth stimulation and evoked potential study in human brain. Cerebral Cortex (New York, N.Y.: 1991) 19 (6), 1462–1473. http://dx.doi.org/10.1093/cercor/bhn18518936272.

Spencer, S.S., 2002. Neural networks in human epilepsy: evidence of and implications for treatment. Epilepsia 43 (3), 219–227. http://dx.doi.org/10.1046/j.1528-1157.2002.26901.x11906505.

Weissenbacher, A., Kasess, C., Gerstl, F., Lanzenberger, R., Moser, E., Windischberger, C., 2009. Correlations and anticorrelations in resting-state functional connectivity MRI: a quantitative comparison of preprocessing strategies. NeuroImage 47 (4), 1408–1416. http://dx.doi.org/10.1016/j.neuroimage.2009.05.00519442749.

Witter, M.P., 1993. Organization of the entorhinal-hippocampal system: a review of current anatomical data. Hippocampus 3 (Spec No 33), 33–448287110.